

Article

Impact of Temperature and Geothermal Gradient on Sandstone Reservoir Quality: the Baiyun Sag in the Pearl River Mouth Basin Study Case (Northern South China Sea)

Chuan Lei ¹, Jinglan Luo ^{1,*}, Xiong Pang ², Chi Li ¹, Jiang Pang ¹ and Yongkun Ma ²

¹ State Key Laboratory of Continental Dynamics, Department of Geology, Northwest University, Xi'an 710069, China; leichuan1988@163.com (C.L.); lichichi123@163.com (C.L.); 18392179630@163.com (J.P.)

² Shenzhen Branch of CNOOC Limited, Shenzhen 518067, China; pangxiong@cnooc.com.cn (X.P.)
mayk4@cnooc.com.cn (Y.M.)

* Correspondence: jlluo@nwu.edu.cn

Received: 4 July 2018; Accepted: 10 October 2018; Published: 15 October 2018



Abstract: Deep-water areas have become a hotspot for global hydrocarbon exploration. In the deep-water area of the Northern South China Sea, a complete set of source rocks, reservoir rocks, and caprock represents a good oil and gas exploration prospect. The Pearl River Mouth basin, an important exploration target in this area, has a wide range of geothermal gradients. However, the mechanism by which the geothermal gradient influences reservoir quality remains unclear, which severely restricts future exploration. We observed that the reduction rates in the porosity and permeability with increasing burial depth and stratum temperature are more rapid in high geothermal gradient areas. The stratum temperature affects the process of diagenesis and the reservoir quality by changing the grain compressive strength, solubility, and precipitation of minerals and clay minerals transformations. With a comparison the crustal extensional thinning histories of different geothermal gradient areas, this study elucidates the comprehensive factors controlling the decreases rates of reservoir porosity and permeability. These findings explain the different evolutions of reservoirs in areas with different geothermal gradients.

Keywords: geothermal gradient; reservoir quality; Pearl River Mouth basin; South China Sea

1. Introduction

Compared to onshore hydrocarbon exploration cost, deep-sea exploration is more expensive. Therefore, reducing risk and cost as much as possible is necessary during offshore oil and gas exploration. While there are relatively few wells currently in deep water areas, understanding the diagenesis processes is necessary for evaluating reservoir quality, deploying further explorations, and improving production efficiencies [1–4]. Temperature directly impacts the processes of diagenesis and reservoir quality [5–7]. Previous studies demonstrate that the properties of reservoirs in different geothermal gradient areas also differ even at the same temperature. [8–13]. At the same temperature, sandstone compaction rates and porosity reduction rates positively correlate with the geothermal gradient. A quantitative calculation method of the compaction rate in different geothermal gradient areas has been previously determined [10]. For sandstone samples with the same composition and degree of sorting, experimental simulation methods were applied to prove positive correlations between the geothermal gradient and the porosity and permeability reduction rate the exists [12]. There are also differences in the diagenetic evolution of sandstones in different geothermal gradient areas in the Baiyun sag and Panyu Low Uplift in the Pearl River Mouth basin (our study area) [13].

However, how the geothermal gradient affects diagenesis and its mechanisms remains unclear. Some scholars posit that higher temperatures increase the rocks' or minerals' internal energy and reduce the cohesion among the particles, which reduces the rock rupture strength [14]. Thus, the rocks or minerals are more susceptible to deformation, and compaction rates increase. Generally, the higher the burial depth is, the worse the sandstone quality is. However, the reservoir quality is different even with the same burial depth/temperature in the Baiyun sag. The factor responsible for this remarkable difference and its mechanism will be discussed in this article.

In recent years, some hydrocarbon discoveries have been made during oil and gas explorations in the Pearl River Mouth basin [15–17]. However, compared with similar basins, such as the Yenggehai Basin in the South China Sea, the Pearl River Mouth basin is still lacking in discoveries of large oil and gas fields. One of the key reasons is that the variation in reservoir permeability is not clear. In the Pearl River Mouth basin, heat flow values increase from the Northwest to the Southeast, with geothermal gradients ranging from 2.87 °C/100 m to 6.47 °C/100 m. The basin therefore provides an excellent opportunity to analyze the evolution of porosity and permeability under conditions of high and low heat fluxes.

At present, there are two contributors to the high heat flow values in the Pearl River Mouth basin: (1) The degree of lithospheric thinning controls the overall trends of heat flow throughout the whole basin [18–22]; and (2) upward migration of hot magmatic fluids along faults due to tectonic activities is the root cause of local abnormal heat fluxes in certain areas [18]. Recent studies have focused on the abnormal heat flow caused by magmatic and hot fluids along faults, which were caused by tectonothermal events in the Baiyun sag [13]. The diagenetic evolution of sandstones within the Zhuhai Group has also been studied with a focus on the compaction and transformation of clay minerals [13]. However, in addition to these certain locations affected by magmatic fluids, faults, and mud diapirs, sandstone reservoirs are also influenced by the basin heat flow caused by widespread lithospheric thinning. Reservoirs that have not been disturbed by deep hot fluids have not been researched.

The present features of the strata are the result of not only the current temperature but also the paleogeothermal state. Temperature has changed continuously throughout geological history. The paleogeothermal gradient of a location is influenced not only by the ancient heat flow but also by the burial history. The physical properties of the sandstones gradually evolved into their current status under the local physical and chemical conditions. If the stratum affected by hydrothermal fluids, the temperature attained in the sediments during their geological history can be different from the present stratum temperature. Therefore, we excluded the samples affected by hydrothermal fluids.

This work aims to understand how geothermal gradient influence reservoir properties and the reasons driving this process. Comprehensive methods were used to determine how reservoir quality evolves within different geothermal gradients, which includes: The composition of the rock skeleton, rock structure, stratum temperature, the geothermal gradient, and the differences in sandstone diagenesis and physical properties. The results provide information for oil and gas explorations in “hot basins” worldwide.

2. Geological Background

The Pearl River Mouth basin is located on the Northern slope of the South China Sea and has water depths of 200 m to 2000 m (Figure 1). As a typical Cenozoic extensional basin, whose stratigraphic record was characterized by fault controlled syn-rift continental sequence and a post-rift marine sequence. It is a petroliferous basin developed on the Caledonian, Hercynian, and Yanshanian deformed basement. From the late Cretaceous to the late Oligocene, the crust of the Northern South China Sea's continental margin was stretched and thinned, forming a series of rift basins, including the Pearl River Mouth basin. The continental Shenhu, Wenchang, Enping, and Zhuhai Groups were deposited during this period. From the late Oligocene to early Miocene, the basin was in a post-extensional stage accompanied by seafloor spreading. The marine Zhujiang, Hanjiang, Yuehai, Wanshan, and Quaternary Groups were deposited during this period.

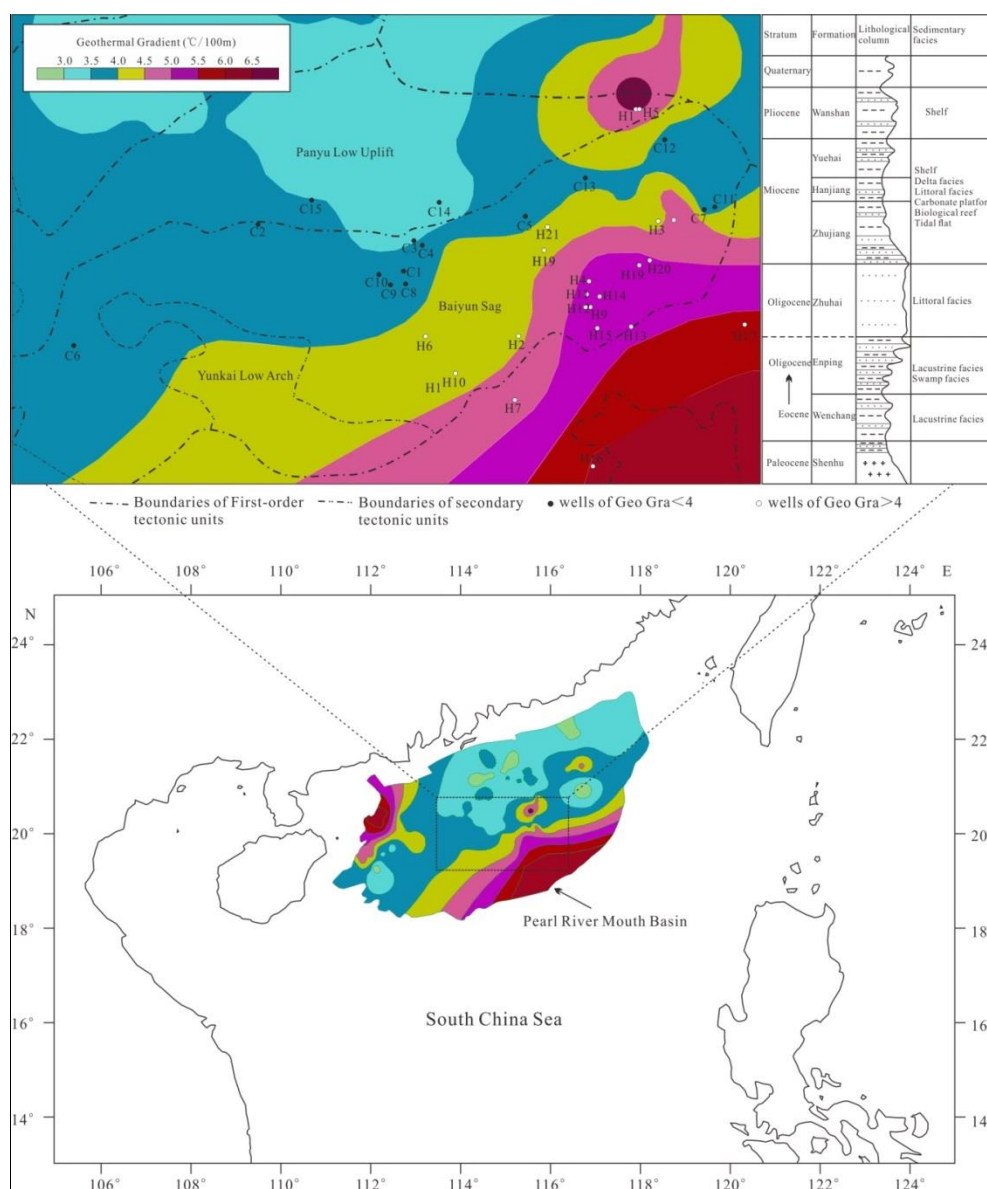


Figure 1. Pearl River Mouth basin in the Northern South China Sea (geothermal gradient distribution modified from Reference [23]).

A cluster of large gas fields has been discovered in the Pearl River Mouth basin, demonstrating the high exploration potential in the deep waters of the South China Sea. The Baiyun sag is approximately 1.206×10^4 km² in area, and its sedimentary thickness is approximately 11,000 m, containing abundant source rock, constituting the largest area and greatest thickness within the Pearl River Mouth basin [17]. This basin is rich in petroleum resources. It is located downstream of the ancient Pearl river system, which transported abundant sand over long distances. Therefore, this region has a great potential for oil and gas exploration [23].

Reports have stated that the surface heat flux of the stable continental margin in the Northern South China Sea is higher than that of the mainland area. The heat flux from the deep mantle accounts for a high percentage of the total heat flow, while the crustal heat flow contributes a lower percentage [24,25]. This pattern is also true within the Pearl River Mouth basin. The thinner the lithosphere, the more heat is transferred from the mantle [18–22].

3. Methodology

The geothermal gradient can be influenced by many other factors, such as lithology, petrophysical properties, formation water activity, and tectonic geological background. The geothermal gradient data used in this study were obtained by correcting the bottom hole temperature (BHT), drill stem test temperature (DST), and modular dynamics formation test (MDT) temperature, which are relatively reliable.

According to the following formula, we calculated the present stratum temperature corresponding to depth as follows:

$$T = T_0 + D \times Gra$$

T —calculated present stratum temperature;

T_0 —the temperature of the sea bottom;

D —burial depth, which is equal to depth minus the water depth and bushing height;

Gra —geothermal gradient.

We select samples from 24 wells, because they were unaffected by hydrothermal fluids, an important criterion for this study. The location of each well is marked on the geological map (Figure 1). There are 12 wells with a geothermal gradient less than 4 °C/100 m (low geothermal gradient) and another 12 wells with a geothermal gradient greater than 4 °C/100 m (high geothermal gradient) among the 24 wells. We avoid wells affected by hydrothermalism (the present stratum temperature is not the highest temperature in the geological history), based on the following criteria: (1) The presence of magmatic activities and the diapiric structures in the through-well seismic profiles; (2) the inclusion homogenization temperature data are higher than the normal stratum temperature; (3) the presence of hydrothermal minerals in the thin sections or SEM images; and (4) the presence of a large proportion of mantle-sourced inorganic carbon dioxide in the natural gas or the presence of visible authigenic dawsonite [26].

Sandstone samples were collected from areas with high and low geothermal gradient. All the samples used in this study are core samples. Based on thin sections, we estimated the contents of skeleton minerals, primary porosity, secondary porosity, and total surface porosity (percentage of the visible pores in two dimensions in whole thin section under microscope) by the visual estimation method. Using a set of standard mineral content patterns as the comparison criteria, the percentage of each fragment was approximately estimated by the observation under a polarizing microscope. An SEM instrument was used to observe the diagenetic characteristics, development of pore types, pore fillers, clay minerals, and other authigenic minerals. XRD mineral composition analysis includes whole-rock and clay-fraction XRD mineral analyses. The XRD method was used to evaluate whether there was any difference in the composition of sandstones from high and low geothermal gradient areas. The content of clay minerals in samples from different depths (temperatures) were obtained to analyze the transformation of clay minerals with the increasing temperature. The porosity and permeability were measured by the helium and air permeability methods, respectively. The samples were washed with alcohol benzene and methanol solvent. Then, rock samples were dried to constant weight at 105 °C after cleaning. The gas expansion method was used to measure the porosity of the rock samples. The skeleton volume was measured by a helium porosimeter. The diameter and length of each sample were measured with a vernier caliper, and the total volume of the sample was calculated. Then, the porosity value was calculated. The air permeability was measured by a permeability apparatus, and the test medium was dry air.

Generally, the quality of a reservoir is determined not only by diagenesis, but also by sedimentation. Reservoir quality is mainly related to the sandstone grain composition, grain size, and sorting. Therefore, the sandstone composition, grain size of sandstone samples from the high and low geothermal gradient areas were compared firstly in this study. Only on the premise that the sedimentary conditions are basically the same, can we compare the differences in diagenesis and analyze the influence of diagenesis on reservoir quality.

4. Results

4.1. Rock Type and Pore Types of the Reservoirs

The sandstone rock types of the Zhujiang, Zhuhai, Enping and Wenchang groups in the study area were divided into several types (Figure 2), according to the thin section observations. The data are shown in Table S1. Samples in the high geothermal gradient area of the Zhujiang Group are mainly composed of arkose, lithic arkose, and quartzarenite. Feldspathic litharenite, litharenite and sublitharenite also occur in small quantities in this group. In the low geothermal gradient area, sandstones of the Zhujiang Group are mainly composed of subarkose and litharenite, followed by feldspathic litharenite and sublitharenite. Samples of the Zhuhai Group are composed of subarkose, sublitharenite, feldspathic litharenite, and lithic arkose in both high and low geothermal gradient areas. The lithic fragment content is high in the Enping Group. The proportions of feldspathic litharenite and litharenite are significantly higher in the Enping Group than in the other groups. Lithic arkose and sublitharenite mainly occur in the Wenchang Group in the high geothermal gradient area, while feldspathic litharenite and litharenite occur mainly in the low geothermal gradient area.

The sandstone types of the Zhuhai group are basically the same in different locations, while those of the Zhujiang, Enping, and Wenchang groups are different. Exception for quartzarenite, other sandstone types in Zhujiang Group are consistent in the high and low geothermal gradient areas (Figure 2). Therefore, we removed the quartzarenite samples of the Zhujiang Group and all samples of the Enping and Wenchang groups to ensure that the rock types of the compared samples are consistent in different locations.

The micro-features of the reservoir pores were determined by petrographic observations (Figures 3–5). Primary pores are mainly intergranular pores—the space between the original framework grains. The secondary pores are mainly dissolution pores. If dissolution can be seen, they were considered to be the secondary pores. Secondary pores are dominated by feldspar dissolution. Primary pores are the main sandstone pore type in the Zhujiang and Zhuhai groups (Figures 3–5). In the low geothermal gradient area, few primary intergranular pores are retained due to the relatively deeper burial depth and stronger mechanical compaction; thus, the proportion of the secondary dissolution pores is relatively high. Significant feldspar dissolution pores are present in the samples (Figure 4A,C), and the intergranular pores are filled with authigenic minerals (mainly authigenic kaolinite and quartz) (Figure 5A,C). In the high geothermal gradient area, the burial depth of the samples is relatively shallow, and the mechanical compaction is relatively weak, and thus the primary intergranular pores are relatively abundant (Figure 4B,D), and the secondary pores are relatively less (Figure 5B,D).

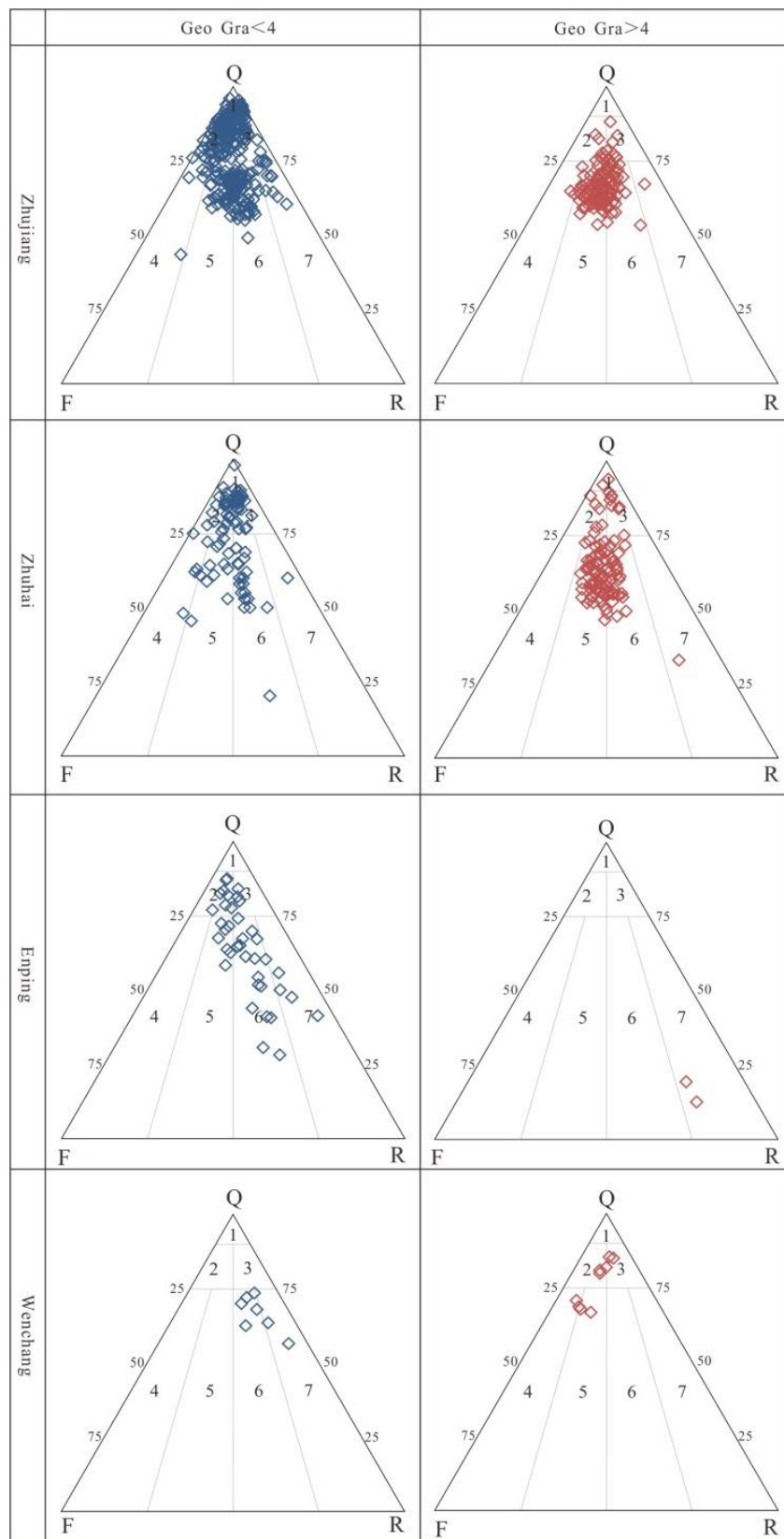


Figure 2. The samples plotted on the QFR (Quartz, Feldspar, Lithic ratios) ternary diagram. (1—Quartzarenite; 2—Subarkose; 3—Sublitharenite; 4—Arkose; 5—Lithic Arkose; 6—Feldspathic Litharenite; and 7—Litharenite). Sandstone classification scheme from Reference [27].

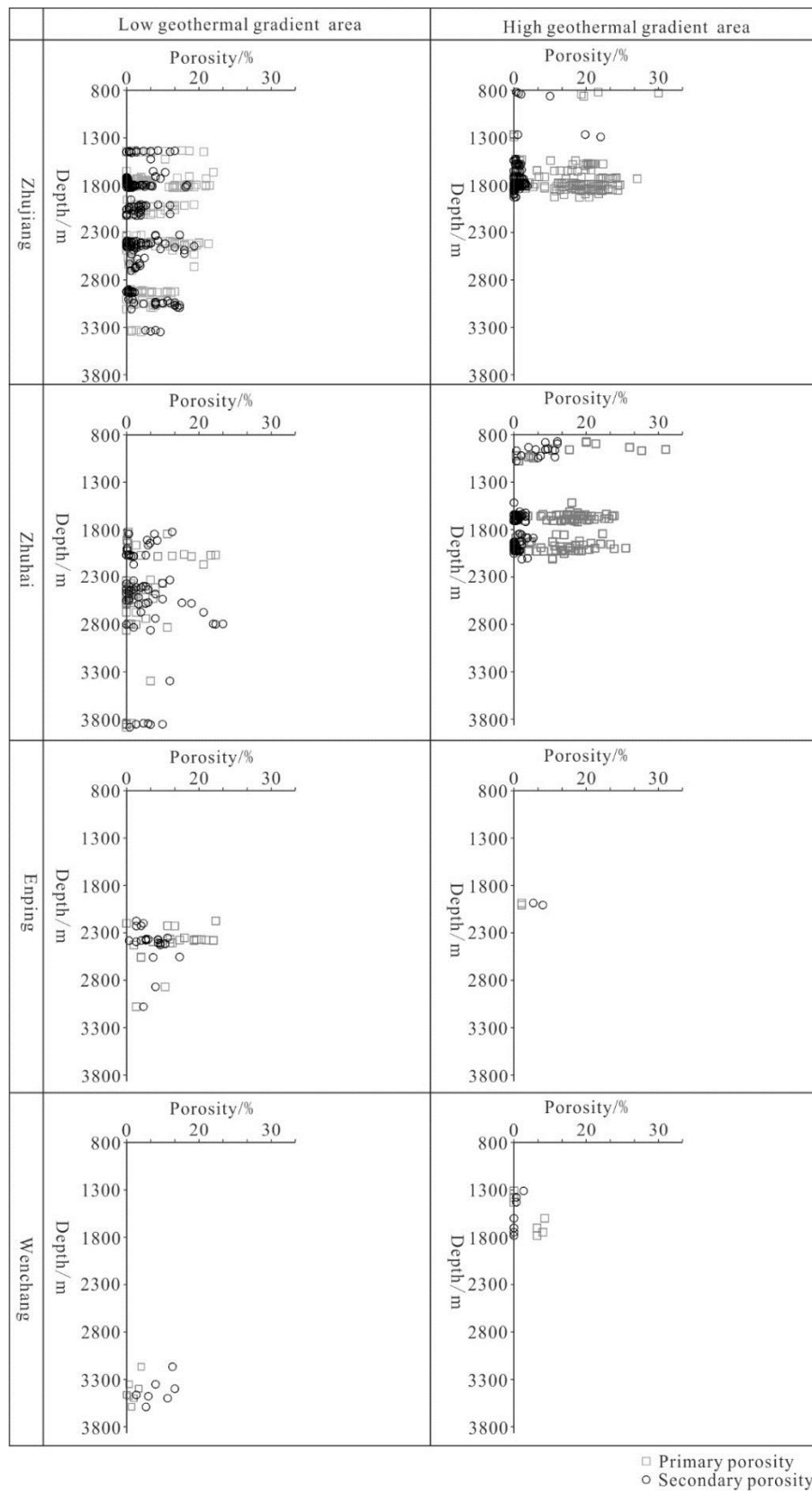


Figure 3. Distribution of primary and secondary pores in the different geothermal gradient areas.

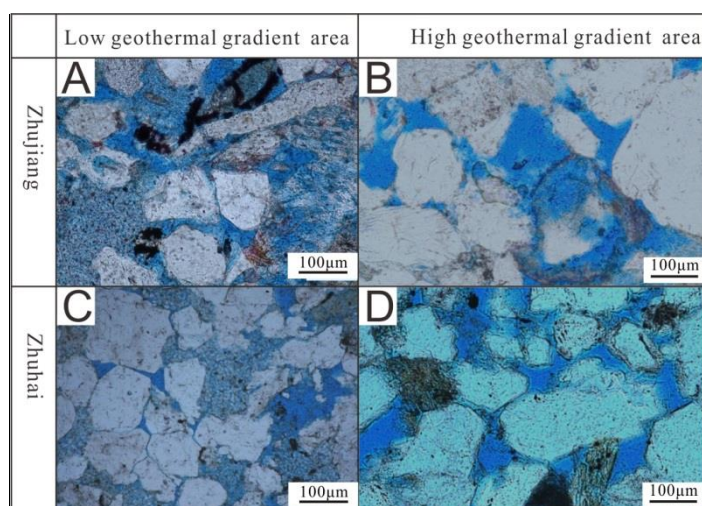


Figure 4. Typical thin-section photomicrographs of pore types in the Baiyun Sag. (A) $Gra = 3.86\text{ }^{\circ}\text{C}/100\text{ m}$, the pore system consists of intergranular pores and feldspar dissolution pores. Kaolinite fills the intergranular pores. (B) $Gra = 4.54\text{ }^{\circ}\text{C}/100\text{ m}$, intergranular pores are the main type of pore. (C) $Gra = 2.87\text{ }^{\circ}\text{C}/100\text{ m}$, dot-line contact, intergranular pores are the main type, but secondary pores are present. (D) $Gra = 4.97\text{ }^{\circ}\text{C}/100\text{ m}$, intergranular pores are the main type of pore.

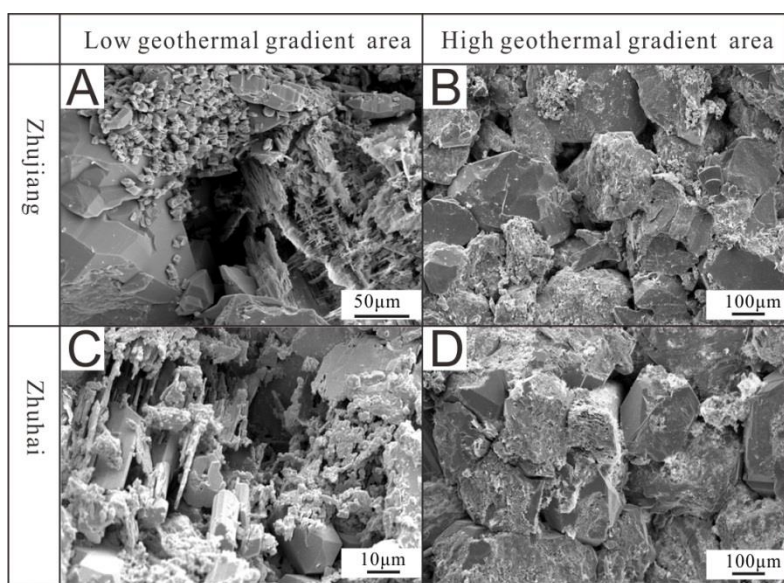


Figure 5. Typical SEM photomicrographs of sandstones in the Baiyun Sag. (A) $Gra = 3.97\text{ }^{\circ}\text{C}/100\text{ m}$, quartz overgrowth and quartz crystal and authigenic kaolinite in intergranular pores. Secondary pores formed by the dissolution of potassium feldspar. (B) $Gra = 4.54\text{ }^{\circ}\text{C}/100\text{ m}$, intergranular pore is the main type of pore. (C) $Gra = 3.93\text{ }^{\circ}\text{C}/100\text{ m}$, the dissolution of feldspar increased the intergranular porosity. Authigenic quartz crystals grew in the pores. (D) $Gra = 4.54\text{ }^{\circ}\text{C}/100\text{ m}$, intergranular pores are the main pore type.

4.2. Grain Size in Different Locations

Generally, grain size of the same sand bodies is characterized by lateral and vertical heterogeneity. To compare the effects of temperature on diagenesis, grain size distributions should be constant. Statistics on the average particle size were determined (Table S2). To compare the grain size between the high and low geothermal gradient areas, we analyzed the distribution of the average grain size of the sandstones at different locations. The average grain size distribution of the sandstone samples from the Zhuhai Group is basically the same in the high and low geothermal gradient areas. We also

calculated the average grain size value for each group. The result shows that there is no difference in the average grain size of the Zhuhai Group in the high (average $\phi = 2.65$) and the low (average $\phi = 2.65$) geothermal gradient areas, while the grain size of the Zhujiang Group in the low geothermal gradient area (average $\phi = 2.17$) is coarser than that in the high geothermal gradient area (average $\phi = 2.84$).

While the grain size of the Zhujiang Group varies in different regions, we do not think that this difference is the main reason for the difference in reservoir quality in different geothermal gradient areas. As there is no direct relationship between grain size and porosity (Figure 6). Therefore, the results of grain size analysis support the discussion in this article.

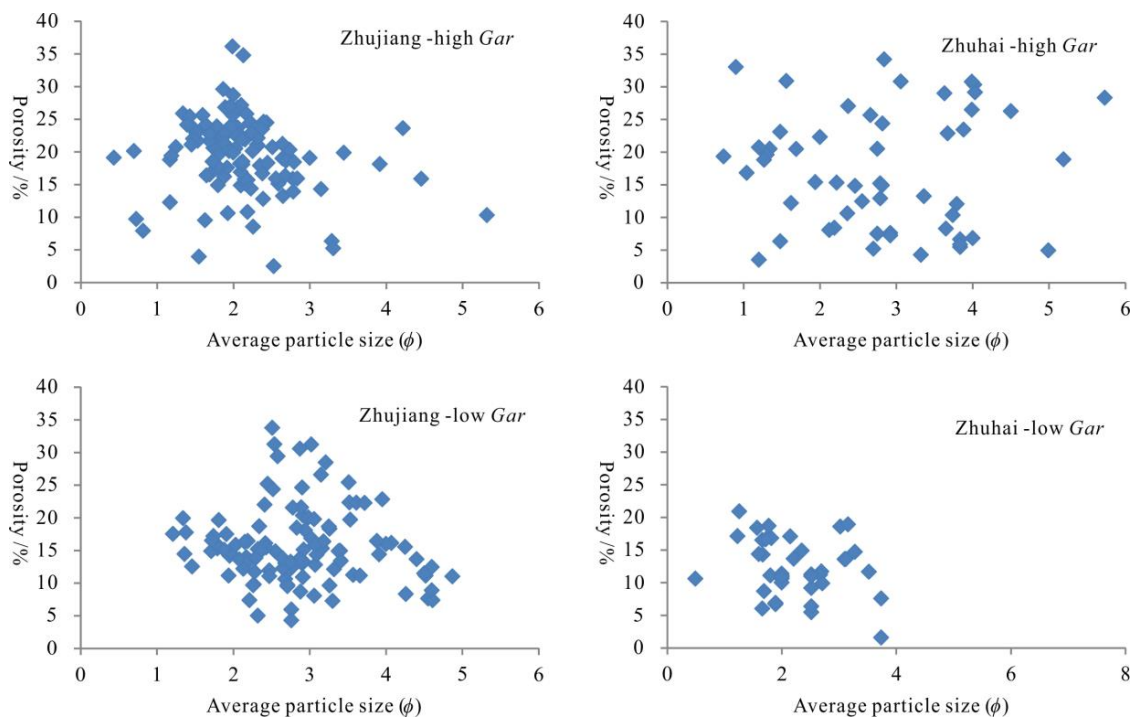


Figure 6. The relation between average grain size and porosity of the Zhujiang and Zhuhai groups in the high and low geothermal gradient (*Gar*) areas.

4.3. Strata Temperature Versus Burial Depth

For the Zhujiang Group, the burial depth in the high geothermal gradient area is relatively shallow (approximately 1412 m on average), while the burial depth in a low geothermal gradient area is deeper (approximately 2983 m on average). The present temperature of a given group in the high geothermal gradient area is lower than that in the low geothermal gradient area. The average crustal thicknesses of the high and low geothermal gradient areas are approximately 17 km and 29 km, respectively [28] (Figure 7). The thinner the crust thickness is, the higher the geothermal gradient.

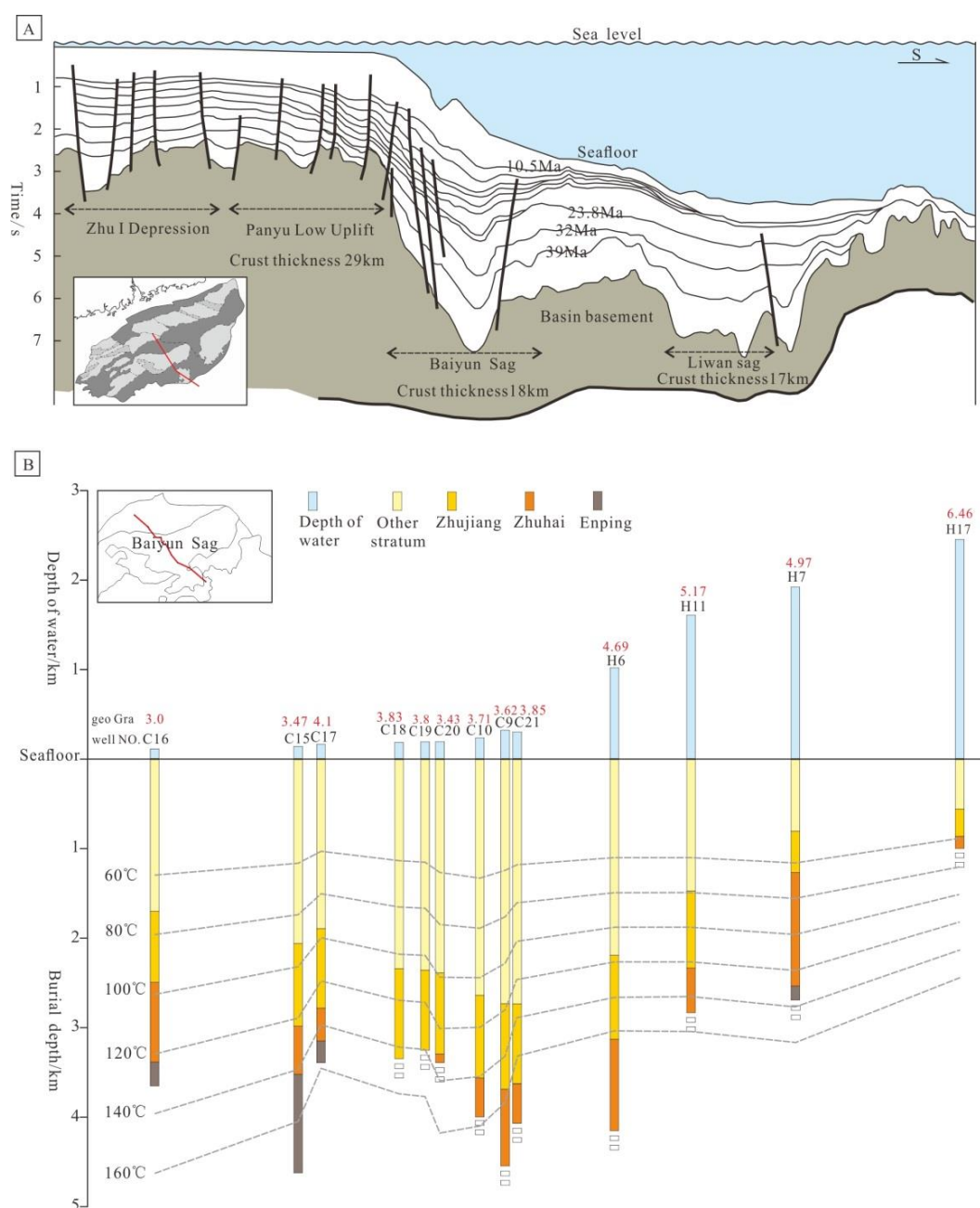


Figure 7. The depth differences between high and low geothermal gradient areas (Figure A modified from Reference [28]). The red line represents the position of the section. (A) Changes in crustal thickness in the geological profile from the Pearl River Mouth basin. (B) Depth difference of iso-temperature curve in the high and low geothermal gradient areas.

4.4. Variation of Porosity and Permeability with Depth/Temperature and Geothermal Gradient

Both permeability and porosity in the research area show a trend of decreasing with temperature and burial depth. The maximum porosity in the low geothermal gradient area is 15% at a depth of approximately 3600 m, and the corresponding temperature is approximately 155 °C. In contrast, the maximum porosity is 15% at a burial depth of approximately 2600 m, with a corresponding temperature of approximately 135 °C in the high geothermal gradient area.

In the low geothermal gradient area, when the sandstone’s permeability is 1 mD, the burial depth is approximately 4300 m, and the corresponding temperature is approximately 175 °C. Whereas,

in the high geothermal gradient area, when the sandstone’s permeability is 1 mD, the burial depth is approximately 2700 m, and the corresponding temperature is approximately 140 °C (Figure 8).

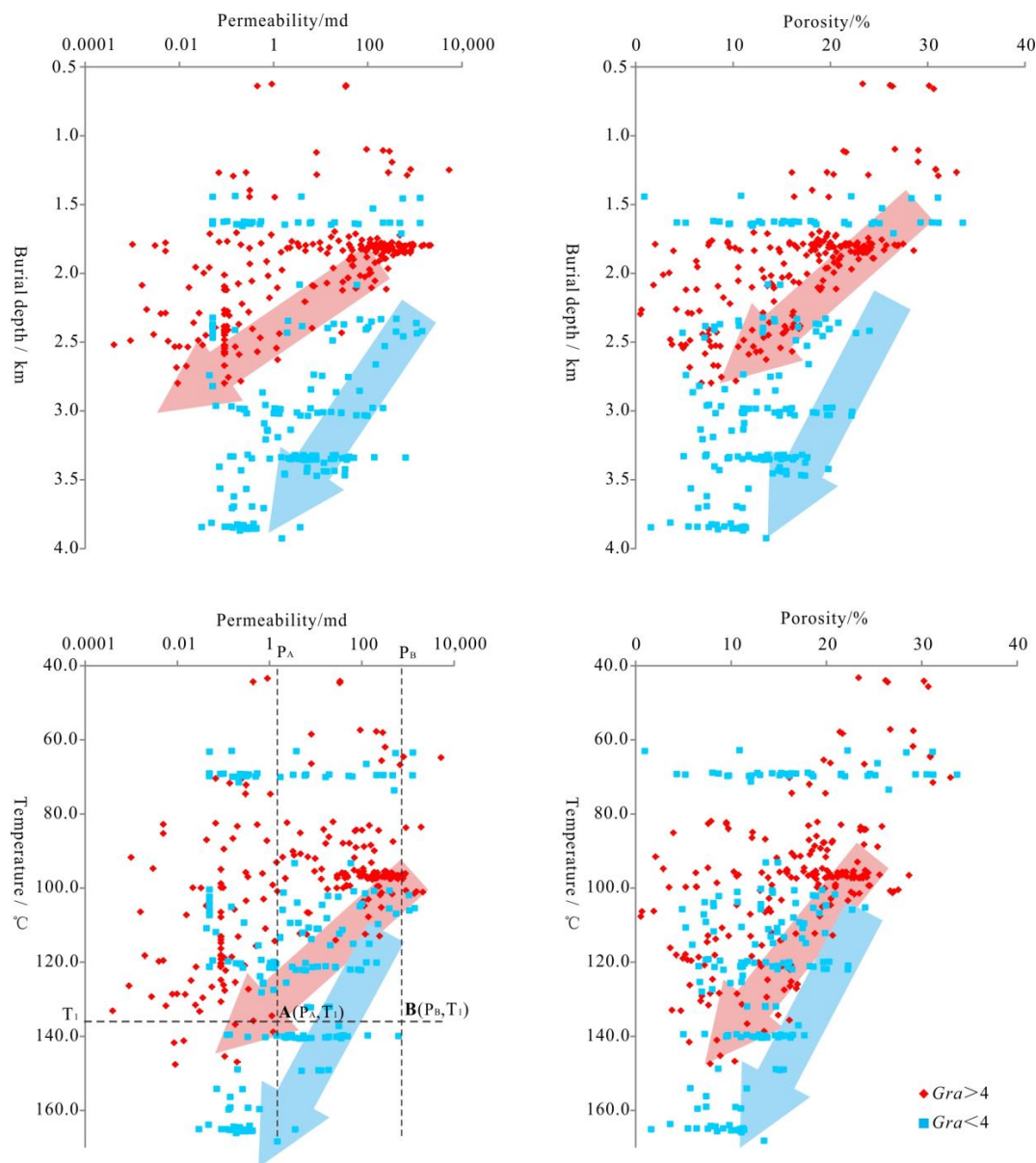


Figure 8. Different trends in porosity/permeability with burial depth/temperature in the high and low geothermal gradient areas.

The maximum porosity reduction rate in the high geothermal gradient area is always greater than that in the low geothermal gradient area whether the burial depth or stratum temperature is used as the ordinate in the figures.

Porosity has negative correlations with burial depth and temperature (Figure 8) in both of the high and low geothermal gradient areas, which is consistent with traditional theory [29,30]. We found that the maximum porosity decreases gradually with the increasing depth in the low geothermal gradient area, but that it decreases rapidly in the high geothermal gradient area. This trend is shown as the different slope of the connection line of maximum porosity (Figure 7). In the high geothermal gradient area, the porosity decreased from 36.1% at 829 m to 11.1% at 2736 m, with an average decrease rate of 1.3110% per hundred meters. While in the low geothermal gradient area, the porosity decreased from 33.7% at 1633 m to 13.5% at 3928 m, with an average decrease rate of 0.9051% per hundred meters

(Figure 8). As a result, at the same burial depth, the porosity and permeability are lower in the high geothermal gradient area than that in the low geothermal gradient area (Figure 8).

In the scatter plot with the stratum temperature as the ordinate, at the same temperature, the difference in maximum porosity (or maximum permeability) between the high and low geothermal gradient areas is small (Figure 8). However, in the high geothermal gradient area, the decrease rate for maximum porosity with the stratum temperature is larger than that in the low geothermal gradient area.

Figure 8 also displays a relationship of permeability vs. stratum temperature. When the temperature is T_1 , the permeability at point A and at point B is P_A and P_B , respectively (Figure 8). In fact, the burial depth of point A is shallower than the depth of point B. Generally, the deeper the burial depth, the stronger the mechanical compaction. Therefore, the P_A should be greater than the P_B . However, the fact is that the P_A is weaker than the P_B (Figure 8).

5. Discussion

5.1. Mechanisms by Which Temperature and Geothermal Gradient Affect Reservoir Quality

A difference was observed in the rates of the maximum porosity and permeability decreases with burial depth between the high and low geothermal gradient areas. At the same burial depth (e.g., 2500–2700 m), the maximum porosity values in the high and low geothermal gradient areas are quite different. Our explanation for this phenomenon is that there were other factors contributing to this difference in addition to the burial depth. We found that at the same temperature, differentiation of the maximum porosity/permeability of sandstones between the high and low geothermal gradient areas is smaller when the temperature is used as the ordinate. Therefore, temperature may be one of the key reasons that attribute to the different rates of maximum porosity/permeability decrease with burial depth. A change in temperature not only affects the physical properties of rocks and minerals but also changes the rates of chemical reactions such as transformation of clay minerals.

5.1.1. Increasing Stratum Temperature Increases Compaction

An increase in temperature enhances the degree of the plasticity of minerals, thus the detrital minerals are easier to occur plastic deformation, which reduce the pressure resistance ability of rocks and enhance the compaction [12,31]. Triaxial compression tests of sandstone show an increase of temperature at constant pressure reduces the yield stress [31]. A rock is more ductile when the temperature increases. Therefore, temperature is an important factor in the compaction of quartz sandstone.

We observe that absolute temperature has an exponential relationship with porosity, while time has a linear relationship with porosity. There is an obvious difference in the degree of compaction between the high and low geothermal gradient areas in the study area. We calculate the original porosity of the reservoir based on the empirical relationship between the original porosity and the sorting coefficient formula by Beard and Weyl [32]. Under the assumption that the volume of rocks decreases in the process of compaction while the volume of skeleton particles remains unchanged, the porosity lost by compaction (COPL) can be calculated by the Ehrenberg's formulas [33]. According to our calculations, at the same burial depth (with different temperatures), the average compaction-related porosity loss is 26.6% and 21.8% for the high and low geothermal gradient area, respectively.

5.1.2. Increasing Stratum Temperature Enhances Quartz Cementation

Generally, an increase in temperature causes an increase in the solubility [34] and precipitation of minerals in the formation water (Figure 9). Consequently, lattice deformation and dissolution of minerals will occur [35–37]. SiO_2 is released into the pore fluid from the dissolution of quartz and clay minerals, saturating the pore water and finally depositing as a quartz overgrowth or as authigenic quartz crystals [38,39]. Quartz cement can fill pore spaces and block pore throats, reducing the porosity and permeability of the reservoir and impeding the development of secondary pores (Figure 9B).

Effective stress data, the temperature history, and the composition and texture of sandstone can be used by geological models to quantitatively calculate the quartz cementation in order to evaluate reservoir properties [4,40,41].

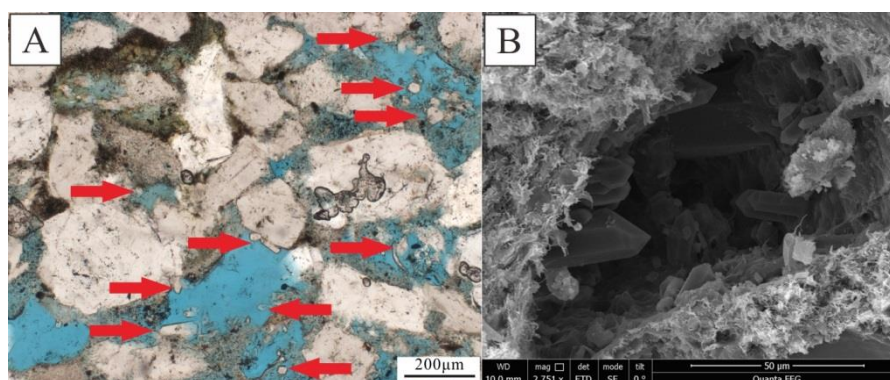


Figure 9. The quartz crystals in pores. (A) Quartz crystals filling in pores of a sandstone in thin section, under plane-polarizing light, indicated by the red arrow. (B) Quartz crystals in the pores of a sandstone under SEM.

5.1.3. Increasing Stratum Temperature Causing Clay Minerals Transformations

Generally, with increasing temperature, the content of smectite and kaolinite decreases, while illite increases. Illite fibers in pores are of bypass growth and can penetrate deeper into pores, thus often fill finer pores and block throats, which causes a greater loss of permeability than any other clay mineral [42]. Illite in the sandstones from the study area shows a negative correlation with both porosity and permeability (Figure 10, Table S3). Filamentous illite divides the original large pores into minor pores or even micropores (Figure 10A,B), which reduce the connectivity between pores dramatically, resulting in a decrease in permeability [43]. In addition, the migration of clay particles will also cause the pore throat to be blocked and finally affect the permeability. Illite, especially with fibrous and filamentous structures (Figure 10A,B), easily breaks up in the fluid flow process, thus producing particle migration [44–46]. The formation of fibrous illite in sandstones can be modeled to predict reservoir quality [42].

The sandstone porosity and permeability show a weak positive correlation with kaolinite content in the Baiyun sag (Figure 10C,D; Table S3), although some samples had high porosity and permeability values with a low content of kaolinite.

There are different points of view regarding how kaolinite affects reservoir properties [47–53]. The first argument holds that under the high-temperature conditions, it is difficult to remove the products of rapid feldspar dissolution [52]. Kaolinite precipitates in situ or nearby, primary intergranular pores in sandstones are converted to micro-intergranular pores between clay minerals, and thus kaolinite does not effectively increase the porosity. The second argument notes that kaolinite is the product of feldspar alteration which is the mark of feldspar dissolution. Kaolinite is also an indicator of a favorable reservoir [54]. The third argument suggests that pores are produced by dissolution and replacement via precipitation of an authigenic mineral equivalent [55]. Whether kaolinite is advantageous or disadvantageous to a reservoir quality depends on the intensity of fluid activity and the closed or open fluid systems in the area. Strong fluid flows can lead to strong fluid migration and lead minerals to deposit in other places. Therefore, strong fluid flows are advantageous to reservoir quality [56].

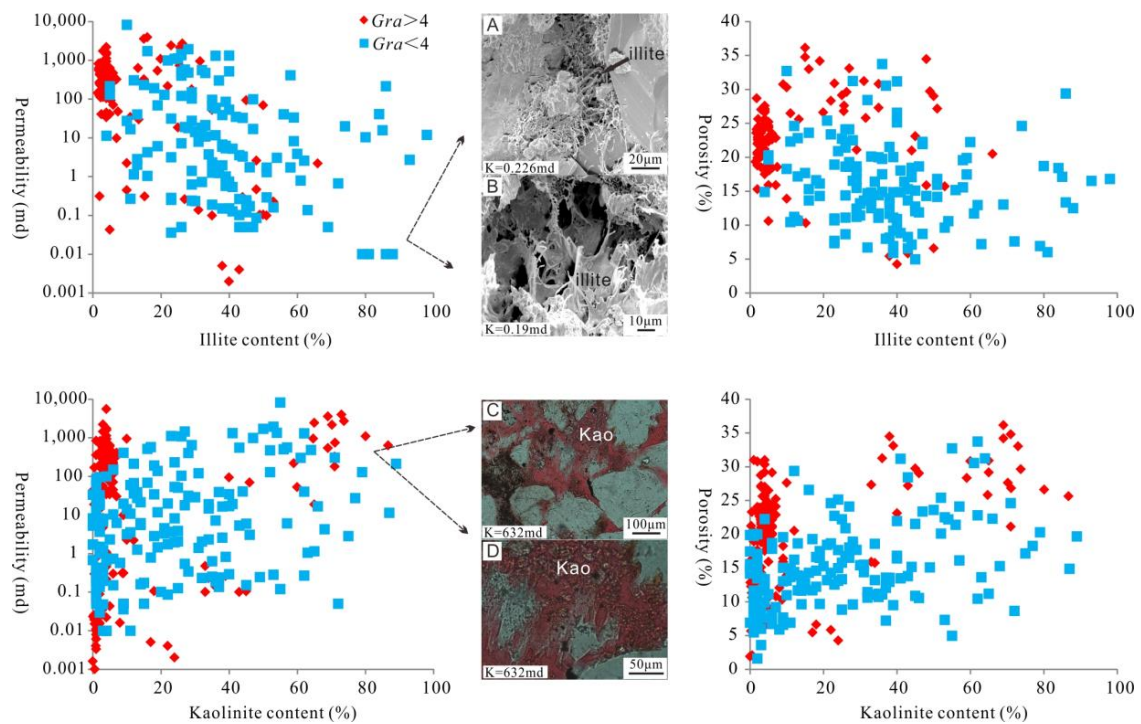


Figure 10. The relationships between clay minerals contents (illite and kaolinite) and reservoir quality.

5.2. Effect of Temporal Factor on the Reservoir Quality

A difference in the reduction rate of the maximum porosity/permeability with stratum temperature between high and low geothermal gradient areas indeed exists, as indicated in Figure 8. If the reduction rates of maximum porosity/permeability are caused by temperature entirely, the maximum porosity/permeability decreasing rates in the high and low geothermal gradient areas should be consistent. However, the stratum temperature is not the only factor causing differences in the reduction rates of porosity and permeability. Heating time should also be taken into account.

The current geothermal gradient does not represent the temperature variation process that the local stratigraphy has experienced throughout its entire geological history. The quality of the reservoir is the result of a geological evolution history. Therefore, the current temperature only represents an instantaneous thermal state. Temporal factor (thermal history) plays an important role on the pore evolution of sandstones. The temporal factor here we mean is that the heating time interval the stratum experienced. The stratum received different amounts of heat and heating interval, when thermal tectonic events occurred at different geological periods.

Similar to the relationship between time and temperature during the kerogen hydrocarbon generation process, temperature and time are also complementary in diagenesis. The same reaction degree can be reached over short period at a high temperature or over long period at a low temperature. Therefore, sandstones experienced a long-term high temperature are more likely to reach a higher reaction degree. The porosity and permeability of the reservoir have decreased less because of the shorter heating time experienced in the low geothermal gradient area, although the burial depth in the low geothermal gradient area is greater. The stratum temperature depends not only on the burial depth but also on the amount of heating from the mantle. The intensity of the heating can be obtained by analyzing the history of the crust thinning of a basin. The high geothermal gradient area in the study has a thin crust (approximately 17 km present) at 23.8 Ma [28], and thus, this area has experienced an intense heat flow at 23.8 Ma. The low geothermal gradient area is located in a region where the crust thickness has always been thicker (approximately 29 km present) and has not experienced intense heat flow.

Taking the horizontal axis as time and the vertical axis as temperature (Figure 11) to predict the reservoir quality, according to the method of thermal evolution path and time-temperature index (TTI) [57], the area restricted by the thermal evolution path and the two coordinates is the value of the TTI (Figure 11). Changes in the burial depth over time reflect uplift and subsidence of the basin. The high geothermal gradient area has experienced a long-term increase in temperature, which is of a high TTI path (Figure 11). While the present stratigraphy in the low geothermal gradient area has a thick burial depth, due to it is far from the mantle and is characterized by a weak heating regime showing as a low TTI path. When the TTI is greater, the final porosity will be lower.

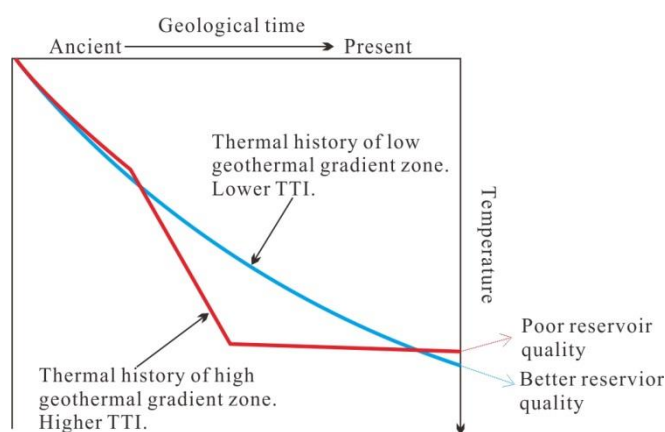


Figure 11. Schematic diagram of the relationship between thermal history and reservoir quality.

6. Conclusions

This work aims to understand the influence of geothermal gradient on sandstone reservoir quality by comparing the features of reservoirs in different geothermal gradient areas. Comprehensive methods were performed for the sandstone sampling from Zhujiang and Zhuhai groups of the Baiyun Sag in the Pearl River Mouth Basin.

(1) The high temperature affects the process of diagenesis and the reservoir quality by enhancing the compaction and cementation, and accelerating the clay mineral transformations in the Baiyun sag.

(2) Temperature and burial duration controls the reduction rates of reservoir porosity and permeability in the Baiyun sag in the Pearl River Mouth basin. More stratum was heated and the longer the heating duration experienced, the faster was the reduction in porosity and permeability. A high time-temperature index value indicates a rapid reduction in porosity and permeability of sandstones. In the Baiyun sag, the stratum in the high geothermal gradient area received more intense heat than that of in the low geothermal gradient area. Therefore, porosity and permeability reducing rates with burial depth/stratum temperature tend to be greater in the high geothermal gradient area than that of the low geothermal gradient area.

(3) We suggest that during the commercial hydrocarbon exploration in the Pearl River Mouth basin, the reservoir temperature and its heating duration in different geothermal gradient areas should be taken into account when evaluating and predicting the favorable reservoirs.

Supplementary Materials: The following are available online at <http://www.mdpi.com/2075-163X/8/10/452/s1>, Table S1: Skeletal mineral composition data of sandstones based on thin section observations, Table S2: The average particle sizes of the Zhujiang and Zhuhai groups in the high and low geothermal gradient areas, Table S3: Data of illite content, kaolinite content, porosity and permeability of samples from the Baiyun Sag.

Author Contributions: C.L. (Chuan Lei) conceived the research rout of this article under the J.L.'s research projects. C.L. (Chuan Lei), C.L. (Chi Li), J.P. and Y.M. collected the samples and data. X.P. and Y.M. provided some scientific research data. C.L. (Chuan Lei) wrote the manuscript under the supervision of J.L. and X.P. J.L. made the final revision of the MS.

Acknowledgments: This research was funded by the National Natural Science Foundation (41572128) and the National Science and Technology Major Project (2016ZX05026003-005). We thank the Shenzhen Branch of CNOOC Limited for providing the core samples and couple of thin sections. The constructive comments made by the reviewers and academic editor are gratefully acknowledged.

Conflicts of Interest: The authors declare no conflict of interest.

References

1. Schmid, S.; Worden, R.H.; Fisher, Q.J. Diagenesis and reservoir quality of the Sherwood Sandstone (Triassic), Corrib Field, Slyne Basin, west of Ireland. *Mar. Pet. Geol.* **2004**, *21*, 299–315. [[CrossRef](#)]
2. Gier, S.; Worden, R.H.; Johns, W.D.; Kurzweil, H. Diagenesis and reservoir quality of Miocene sandstones in the Vienna Basin, Austria. *Mar. Pet. Geol.* **2008**, *25*, 681–695. [[CrossRef](#)]
3. Dutton, S.P.; Loucks, R.G. Diagenetic controls on evolution of porosity and permeability in lower Tertiary Wilcox sandstones from shallow to ultradeep (200–6700m) burial, Gulf of Mexico Basin, U.S.A. *Mar. Pet. Geol.* **2010**, *27*, 1775–1787. [[CrossRef](#)]
4. Lander, R.H.; Laubach, S.E. Insights into rates of fracture growth and sealing from a model for quartz cementation in fractured sandstones. *Geol. Soc. Am. Bull.* **2015**, *127*, 516–538. [[CrossRef](#)]
5. Aruna, M. The Effects of Temperature and Pressure on Absolute Permeability of Sandstones. Ph.D. Thesis, Stanford University, Stanford, CA, USA, 1976.
6. Schembre, J.M.; Kovscek, A.R. Mechanism of Formation Damage at Elevated Temperature. *J. Energy Resour. Technol.* **2005**, *127*, 171–180. [[CrossRef](#)]
7. Hassanzadegan, A.; Blöcher, G.; Zimmermann, G.; Milsch, H. Thermoporoelectric properties of Flechtinger sandstone. *Int. J. Rock Mech. Min. Sci.* **2012**, *49*, 94–104. [[CrossRef](#)]
8. Dixon, S.A.; Kirkland, D.W. Relationship of temperature to reservoir quality for feldspathic sandstones of southern California. *AAPG Bull.* **1985**, *69*, 82–99.
9. Jiang, T.; Xie, X. Effects of high temperature and overpressure on reservoir quality in the Yinggehai basin, South China Sea. *J. Earth Sci.* **2005**, *30*, 215–220. (In Chinese)
10. Shou, J.; Zhang, H.; Shen, Y.; Wang, X.; Zhu, G.; Si, C. Diagenetic mechanisms of sandstone reservoirs in China oil and gas-bearing basins. *Acta Petrol. Sin.* **2006**, *22*, 2165–2170. (In Chinese)
11. Fisher, Q.J.; Harris, S.D.; Casey, M.; Knipe, R.J. Influence of grain size and geothermal gradient on the ductile-to-brittle transition in arenaceous sedimentary rocks: Implications for fault structure and fluid flow. *Geol. Soc. Lond. Spec. Publ.* **2007**, *289*, 105–121. [[CrossRef](#)]
12. Hou, G.; Ji, Y.; Wu, H.; Li, L.; Wang, Y.; Wang, W. Quantitative Characterization on the Influence Factors of Porosity and Permeability Characteristics of Clastic Reservoirs by Physical Experiment Simulation. *Geol. Sci. Technol. Inf.* **2017**, *4*, 153–159. (In Chinese)
13. Li, C.; Luo, J.; Hu, H.; Chen, S.; Wang, D.; Liu, B.; Ma, Y.; Chen, L.; Li, X. The thermodynamic impact on deepwater sandstone diagenetic evolution of the Zhuhai Group in Baiyun Sag, Pearl River Mouth Basin. *J. Earth Sci.* **2018**. (In Chinese)
14. Hu, L. *An Overview of Microstructural Geology*; Geological Publishing House: Beijing, China, 1998. (In Chinese)
15. Zhu, W.; Zhong, K.; Li, Y.; Xu, Q.; Fang, D. Characteristics of hydrocarbon accumulation and exploration of the northern South China Sea deep-water basins. *Chin. Sci. Bull.* **2012**, *57*, 1833–1841. (In Chinese)
16. Shi, H.; He, M.; Zhang, L.; Yu, Q.; Pang, X.; Zhong, Z.; Liu, L. Hydrocarbon geology, accumulation pattern and the next exploration strategy in the eastern Pearl River Mouth basin. *China Offshore Oil Gas* **2014**, *26*, 11–22. (In Chinese)
17. Zhang, G.; Yang, H.; Chen, Y.; Ji, M.; Wang, K.; Yang, D.; Han, Y.; Sun, Y. The Baiyun Sag: A giant rich gas-generation sag in the deepwater area of the Pearl River Mouth Basin. *Nat. Gas Ind.* **2014**, *34*, 11–25. (In Chinese)
18. Mi, L.; Yuan, Y.; Zhang, G.; Hu, S.; He, L.; Yang, S. Characteristics and Genesis of Geothermal Field in Deep-water Area of the Northern South China Sea. *Acta Pet. Sin.* **2009**, *30*, 27–33. (In Chinese)
19. Song, Y.; Zhao, C.; Zhang, G.; Song, H.; Shan, J.; Chen, L. Research on tectono-thermal modeling for Qiongdongnan Basin and Pearl River Mouth Basin in the northern South China Sea. *Chin. J. Geophys.* **2011**, *54*, 3057–3069. (In Chinese)

20. McKenzie, D. Some remarks on the development of sedimentary basins. *Earth Planet. Sci. Lett.* **1978**, *40*, 25–32. [[CrossRef](#)]
21. Royden, L.; Keen, C.E. Rifting process and thermal evolution of the continental margin of Eastern Canada determined from subsidence curves. *Earth Planet. Sci. Lett.* **1980**, *51*, 343–361. [[CrossRef](#)]
22. Keen, C.E.; Dehler, S.A. Stretching and subsidence: Rifting of conjugate margins in the North Atlantic Region. *Tectonics* **1993**, *12*, 1209–1229. [[CrossRef](#)]
23. Mi, L.; Liu, B.; He, M.; Pang, X.; Liu, J. Petroleum geology characteristics and exploration direction in Baiyun deep water area, northern continental margin of the South China Sea. *China Offshore Oil Gas* **2016**, *28*, 10–22. (In Chinese)
24. Zhang, J.; Wang, J. Deep geothermal characteristics of the continental margin, the northern South China Sea. *Chin. Sci. Bull.* **2000**, *45*, 1095–1100. (In Chinese)
25. Tang, X.; Yang, S.; Zhang, G.; Liang, J.; Shan, J.; Zhuang, W.; Hu, S. Overview on geothermal investigation of the South China Sea. *Prog. Geophys.* **2013**, *28*, 988–997. (In Chinese)
26. Lei, C.; Luo, J.; Ma, Y.; Li, C.; Zhang, L.; Pang, J.; Li, X. Distribution of Carbon Dioxide in Baiyun Sag and its Periphery, Pearl River Mouth Basin. *J. Mineral. Petrol.* **2017**, *37*, 97–106. (In Chinese)
27. Folk, R. *Petrology of Sedimentary Rocks*; Hemphill Publishing Ltd.: Sutton, UK, 1980.
28. Pang, X.; Chen, C.; Peng, D.; Zhou, D.; Shao, L.; He, M.; Liu, B. Basic geology of Baiyun deep-water area in the northern South China Sea. *China Offshore Oil Gas* **2008**, *20*, 215–222. (In Chinese)
29. Atwater, G.I.; Miller, E.E. The effect of decrease in porosity with depth on future development of oil and gas reserves in south Louisiana: Abstract. *AAPG Bull.* **1965**, *49*, 334.
30. Ehrenberg, S.N. Relationship between diagenesis and reservoir quality in sandstones of the Garn Formation, Haltenbanken, Mid-Norwegian Continental Shelf. *AAPG Bull.* **1990**, *74*, 1538–1558. [[CrossRef](#)]
31. Handin, J.W.; Hager, R.V. Experimental deformation of sedimentary rocks under confining pressure: Tests at high temperature. *AAPG Bull.* **1958**, *42*, 2892–2934. [[CrossRef](#)]
32. Beard, D.C.; Weyl, P.K. Influence of texture on porosity and permeability of unconsolidated sand. *AAPG Bull.* **1973**, *57*, 349–369.
33. Ehrenberg, S.N. Assessing the relative importance of compaction processes and cementation to reduction of porosity in sandstones: Discussion; compaction and porosity evolution of pliocene sandstones, Ventura Basin, California: Discussion. *AAPG Bull.* **1989**, *73*, 1274–1276.
34. Liu, B.; Zhang, J. *Sedimentary Diagenesis*; Science Press: Beijing, China, 1992. (In Chinese)
35. Mitra, S.; Beard, W.C. Theoretical models of porosity reduction by pressure solution for well-sorted sandstones. *J. Sediment. Res.* **1980**, *50*, 1347–1360.
36. Feng, Z. *Sedimentology*; Petroleum Industry Press: Beijing, China, 1993. (In Chinese)
37. Liu, G.; Jin, Z.; Zhang, L. Simulation Study on Clastic Rock Diagenetic Compaction. *Acta Sedimentol. Sin.* **2006**, *24*, 407–413. (In Chinese)
38. Cyziene, J.; Molenaar, N.; Sliupa, S. Clay-induced pressure solution as a Si source for quartz cement in sandstones of the Cambrian Deimena Group. *Geologija* **2006**, *53*, 8–21.
39. Metwally, Y.M.; Chesnokov, E.M. Clay mineral transformation as a major source for authigenic quartz in thermo-mature gas shale. *Appl. Clay Sci.* **2012**, *55*, 138–150. [[CrossRef](#)]
40. Lander, R.H.; Walderhaug, O. Predicting porosity through simulating sandstone compaction and quartz cementation. *AAPG Bull.* **1999**, *83*, 433–449.
41. Lander, R.H.; Larese, R.E.; Bonnell, L.M. Toward more accurate quartz cement models: The importance of euhedral versus noneuhedral growth rates. *AAPG Bull.* **2008**, *92*, 1537–1563. [[CrossRef](#)]
42. Lander, R.H.; Bonnell, L.M. A model for fibrous illite nucleation and growth in sandstones. *AAPG Bull.* **2010**, *94*, 1161–1187. [[CrossRef](#)]
43. Muecke, T.W. Formation fines and factors controlling their movement in porous media. *J. Pet. Technol.* **1979**, *31*, 144–150. [[CrossRef](#)]
44. Stalder, P.J. Influence of crystallographic habit and aggregate structure of clay mineral on sandstone permeability. *Geol. Mijnb.* **1973**, *52*, 217–220.
45. Khilar, K.C.; Fogler, H.S.; Ahluwalia, J.S. Sandstone water sensitivity: Existence of a critical rate of salinity decrease for particle capture. *Chem. Eng. Sci.* **1983**, *38*, 789–800. [[CrossRef](#)]
46. Worden, R.H.; Morad, S. Controls on formation, distribution and evolution. In *Clay Mineral Cements in Sandstones*; Blackwell Science: Hoboken, NJ, USA, 2003; pp. 3–41.

47. Nagy, K.L.; Blum, A.E.; Lasaga, A.C. Kaolinite precipitation and dissolution: Effects on porosity and permeability. In Proceedings of the AAPG annual convention with DPA/EMD Divisions and SEPM, San Antonio, TX, USA, 23–26 April 1989.
48. Morad, S.; Ismail, H.N.B.; Ros, L.F.D.; Al-Aasm, I.S.; Serrhini, N.E. Diagenesis and formation water chemistry of Triassic reservoir sandstones from southern Tunisia. *Sedimentology* **1994**, *41*, 1253–1272. [[CrossRef](#)]
49. Osborne, M. Variation in Kaolinite Morphology with Growth Temperature in Isotopically Mixed Pore-Fluids, Brent Group, UK North Sea. *Clay Min.* **1994**, *29*, 591–608. [[CrossRef](#)]
50. Hassouta, L. Clay Diagenesis in the Sandstone Reservoir of the Ellon Field (Alwyn, North Sea). *Clay Clay Min.* **1999**, *47*, 269–285. [[CrossRef](#)]
51. Cao, J.; Zhang, Y.; Hu, W.; Zhang, Y.; Tang, Y.; Yao, S.; Tao, G. Developing characteristics of kaolinite in central Junggar basin and their effect on the reservoir quality. *Acta Mineral. Sin.* **2005**, *25*, 367–373. (In Chinese)
52. Wilson, M.J.; Wilson, L.; Patey, I. The influence of individual clay minerals on formation damage of reservoir sandstones: a critical review with some new insights. *Clay Min.* **2016**, *49*, 147–164. [[CrossRef](#)]
53. Yuan, G.; Cao, Y.; Xi, K.; Wang, Y.; Li, X.; Yang, T. Feldspar dissolution and its impact on physical properties of Paleogene clastic reservoirs in the northern slope zone of the Dongying sag. *Acta Pet. Sin.* **2013**, *34*, 853–866. (In Chinese)
54. Fu, W. Influence of Clay minerals on Sandstone Reservoir Properties. *J. Palaeogeogr.* **2000**, *2*, 59–68. (In Chinese)
55. Zhu, G. Effects of Clay Minerals on the Triassic Sandstone Reservoir in Shan-Gan-Ning Basin and Their Significance. *Pet. Explor. Dev.* **1988**, *4*, 20–29. (In Chinese)
56. Mc Laughlin, O.M.; Mc Aulay, G.E.; Haszeldine, R.S. Deep to shallow kaolinite relocation generates porosity. In Proceedings of the Annual convention of the American Association of Petroleum Geologists, Inc. and the Society for Sedimentary Geology: Global exploration and geotechnology, San Diego, CA, USA, 19–22 May 1996.
57. Shou, J.; Zhang, H.; Si, C.; Wang, X.; Chen, Z.; Wang, S. *Sandstone Dynamic Is Digenesis*; Petroleum Industry Press: Beijing, China, 2005. (In Chinese)



© 2018 by the authors. Licensee MDPI, Basel, Switzerland. This article is an open access article distributed under the terms and conditions of the Creative Commons Attribution (CC BY) license (<http://creativecommons.org/licenses/by/4.0/>).